Numerical Study on Ground Subsidence Due to Crushing Single Isolated Boulder by Tunnelling

Ye Lu[1(✉)], Yong Tan[2(✉)], Wanlei Chen[2], Fangle Peng[2], Shaoming Liao[2], Xianghua Song[2], and Weizhen Jiang[2]

[1] Shanghai University, Shanghai, China
[2] Tongji University, Shanghai, China
tanyong2lth@tongji.edu.cn

Abstract. Distinct from shield tunnelling in clayey and sandy strata, crushing undetected single isolated boulder by tunnelling machine frequently resulted in severe ground subsidence hazards (e.g., cave-in of ground). These ground subsidence usually happened suddenly with little warning, occurred few hours to few years post-tunnelling, and did not feature a continuous settlement trough curve like those of tunnelling in fine grained soils. In light of these, it is extremely difficult to predict potential ground subsidence hazards and then to adopt appropriate countermeasures or post-tunnelling remedial measures to prevent associated damages. By applying a systematic methodology that can randomly yield close approximation of morphology of rock blocks into commercial particle flow code PFC2D, the influence of boulder location on ground settlements, overburden pressures, and bending moments in the tunnel lining was investigated. The numerical simulations disclosed that the shape of ground settlements trough reflected the location of crushed boulder. In the meantime, crushing and removing the boulder would change earth pressure around the tunnel and thus caused the bending moments in the lining to redistribute.

Keywords: Tunnelling · Boulder · Ground settlements

1 Introduction

Till 2019, more than 4000 km underground transit lines have been built in approximate forty cities of China. For metro lines buried in soil strata, they were usually constructed by shield tunnelling method. In recent years, unfavorable geological conditions, e.g., large single isolated boulder in soil strata, were frequently encountered during shield tunnelling, which incurred tremendous problems for tunnelling work, e.g., damaging tunnelling machine and significant ground settlement [1]. For the moment, there are several methods developed for crushing boulder [2–5], e.g., blasting boulder by surface drilling, surface punching, and removal of boulder within an excavation shaft. In practice, boulders are randomly located in strata, which are very difficult to be detected or located in advance using current geophysical methods. Thereby, in most cases boulder was unable to be detected until tunnelling machine arrived at its location. In such case, the boulder can be shattered by drilling and splitting from excavation

A. G. Correia et al. (Eds.): ICITG 2019, SSGG, pp. 889–896, 2020.
https://doi.org/10.1007/978-3-030-32029-4_75

chamber of tunneling machine. However, this action would cause project delay and even instability of excavation face followed by significant ground subsidence. Because of this, in case cutterhead of tunnelling machine had strong rock-cutting ability, the boulder was often crushed directly by an advancing TBM without stop. However, crushing an oversized boulder, in particular those extending past TBM perimeter, could lead to excessive ground loss, featured by pronounced ground subsidence or even destructive cave-in of roadway. Unfortunately, until now few studies have been known in literature for characterizing ground subsidence and exploring associated failure mechanism due to crushing boulder by shield tunnelling, although relevant ground subsidence accidents have been frequently reported in practice. This made it difficult for engineers to prevent or mitigate relevant risks by preparing suitable countermeasures in advance.

Because of these concerns, this study intends to explore ground subsidence associated with crushing boulder by tunnelling in sand strata. For the examined geological condition, both boulder and sand grains feature obvious discrete characteristics. Because discrete-element-method (DEM) can capture microscopic behaviors of boulder-sand mixtures [6, 7], the commercial DEM software, particle-flow-code (PFC2D), was adopted in this study for investigation. The basic elements in PFC2D are circular disks only and unable to accurately capture mechanical behaviors of boulder-sand mixtures, which are closely related to morphology and size of boulder. Considering this, an integrated computational approach [8] for simulating irregularly shaped rock blocks was implemented into PFC2D for simulation first; then, extensive numerical parametric studies were conducted to explore the influences of location of boulder along tunnel circumference and volume loss of ground. Finally, conclusions and suggestions based on the numerical analyses were drawn.

2 Numerical Simulation of Tunnel and Soils

The tunnel modeled was 6.0 m in diameter and its concrete lining was 0.6 m in thickness. In order to enable its displacements and deformations, the lined tunnel was simulated using multiple single disks bonded by parallel bonds. 60 spherical disks with diameter of 0.66 m were used to simulate tunnel lining, and parallel bonds with 0.6 m in diameter were assigned to bond the disks together. To calibrate the numerical parameters for the tunnel, numerical estimation of tunnel deflections being subjected to a single point load of 100 kN were compared with the values estimated by virtual work theory. δ_1 is the vertical deflection at tunnel vault and δ_2 is the lateral deflection at tunnel side wall. The calibrated numerical parameters for the tunnel are listed in Table 1, and the computed tunnel deflections are listed in Table 2.

The soil stratum simulated was sand with isolated boulders. Sand particles were simulated using single spheres which were generated in a box with 40 m $\times$ 40 m in dimension, and they were equilibrated under gravitational force of 1 g. Then, a single boulder was positioned in the sands. The boulder was created using the computational methodology proposed by Lu et al. [8]. After generation of the single boulder, the ground surface was leveled to make the stratum thickness of 33 m, see Fig. 1a. As introduced previously, if a large-sized boulder extending past TBM perimeter is

crushed by the cutter-head, severe ground subsidence or cave-in of roadway might be incurred. Therefore, such scenario was considered in the current study. It was simulated by deleting the single boulder and sand particles within the scope of tunnel, and then tunnel lining was added (Fig. 1b). The cover depth of tunnel, C, was 12 m and tunnel diameter was 6 m, which resulted in a cover to diameter ratio of 2.0. The volume losses due to over-excavation and crushed boulder were 5% and 25%, which led to a total volume loss, R_s, of 30%. The model was cycled to let the ground surface to cave in and finally reached equilibrium state (unbalanced particle force was less than 1×10^{-5} N), see Fig. 1c.

Table 1. Numerical parameters used in DEM modeling.

Parameters	Sand	Boulder	Tunnel lining	Wall
Specific gravity	2.6	2.7	2.5	–
Particle friction coefficient	0.7	0.7	–	0.5
Particle normal stiffness, N/m	5.0×10^7	8.0×10^8	5.8×10^9	1.0×10^9
Particle shear stiffness, N/m	5.0×10^7	8.0×10^8	5.9×10^9	1.0×10^9
Normal stiffness of parallel bond, Pa/m	–	–	4.95×10^{11}	–
Shear stiffness of parallel bond, Pa/m	–	–	3.3×10^{11}	–
Normal strength of parallel bond, Pa	–	–	1.0×10^9	–
Shear strength of parallel bond, Pa	–	–	1.0×10^9	–
Radius multiplier for parallel-bond radius	–	–	0.91	–

Table 2. Tunnel deflections computed by analytical solution and numerical modeling.

Tunnel deflection	Analytical method (mm)	Numerical modeling (mm)
δ_1	3.0995	3.1702
δ_2	2.8462	2.8356

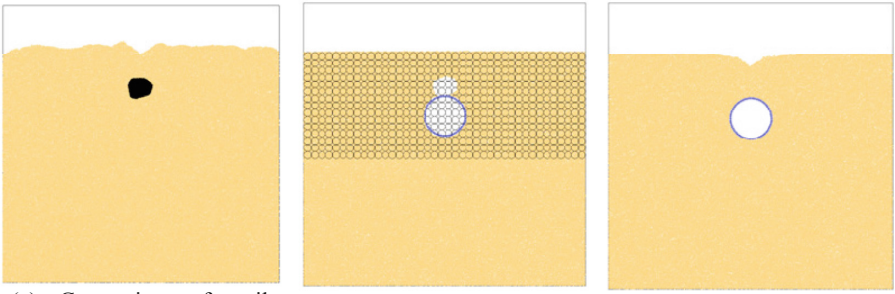

(a) Generation of soil stratum (b) Excavation of tunnel (c) Ground cave-in

Fig. 1. Setup of numerical model for tunnel excavation.

3 Modeling Results

In this study, ground settlements, overburden pressures and bending moments of tunnel lining were investigated for crushing a single boulder located at different places around the tunnel. Here, a location angle, α, was defined in Fig. 2. Due to the axis-symmetry of the numerical model, α varies between 0°–180°. α = 0° refers to the case that the boulder is located on the tunnel crown, and α = 180° refers to the case when the boulder is located below the tunnel invert.

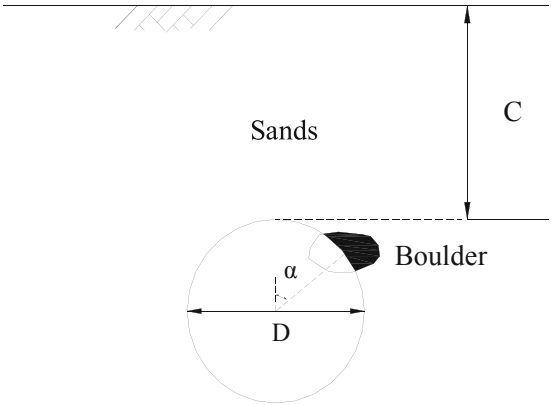

Fig. 2. Illustration of location angle of boulder.

3.1 Contact Forces Between Particles

Figure 3 shows contact forces between particles and deformation of soil stratum after the boulder at α = 45° was crushed and tunnel lining was installed. The contact forces between particles are referred to normal forces occurred in the contact points, and are represented by black lines in Fig. 3. It can be seen from the figure that the particle contact forces in the sand stratum atop the cavity had diminished shortly after the lining was installed (Fig. 3a), which indicates a loosening zone was formed atop the cavity. At this time point, the sand particles barely maintained their positions, which should be ascribed to that friction and interlocking forces still overrode gravity forces. As time passed by, sand particles started to fall down due to gravity and filled up the cavity (Fig. 3b). During this stage, the loosening zone decreased, and the scope of falling zone moved up until it reached the ground surface (Fig. 3c). Then, the ground surface started to cave in drastically, and the cave-in depth increased and the scope of influence zone extended (Fig. 3d).

3.2 Ground Settlements

Figure 4 plots the ground settlement troughs caused by crushing the boulder at different locations. In the figure, X is the distance from tunnel center. As expected, the location of

the maximum ground settlement was relevant to the location of crushed boulder. When the crushed boulder was located right atop the tunnel crown, the maximum ground settlement was up to 65 cm and occurred at X/D = 0. When the boulder located at the right wing of the tunnel was crushed, the maximum settlement of 38 cm occurred at 1D distance away from tunnel center. It is interesting to note that the maximum settlement maintained around the tunnel center for $\alpha = 135°$ and 180°. This can be explained by that when $\alpha > 90°$, the cavity resulting from boulder removal were filled up by soils from both right and left wings of the tunnel, which reflected to the ground surface as a settlement trough with the maximum settlements occurred at the tunnel center.

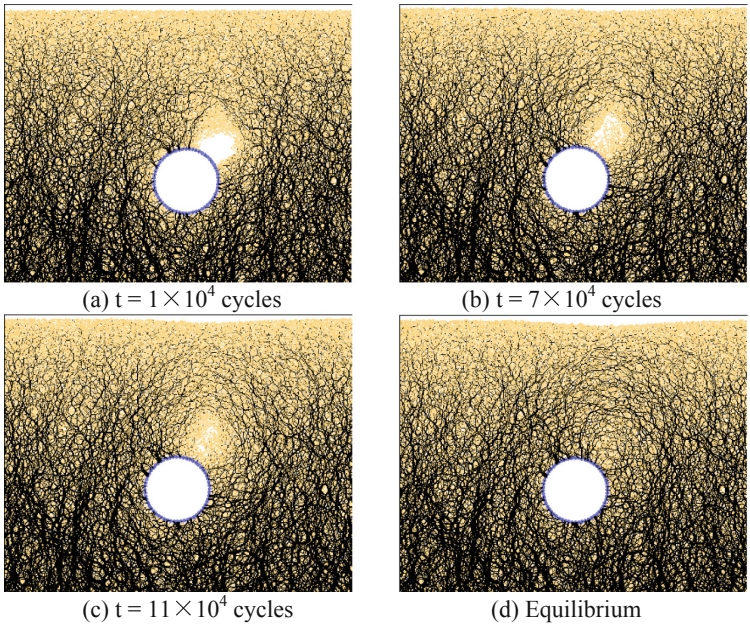

Fig. 3. Evolution of contact forces between soil particles during ground cave-in.

3.3 Overburden Pressures

As a tunnel is buried in the soil, it is subjected to overburden pressures after the lining is installed. Some measurement circles with diameter of 1 m were placed in the soil layer to measure the pressures (see Fig. 1b). Figure 5 plots the overburden pressures when the stratum regained equilibrium after removal of the boulder. In general, the distribution curves of overburden pressures were not flat, which should be ascribed to the discrete behaviors of particles in PFC simulation. It can be seen from the figure that removal of the boulder resulted in decrease of overburden pressure around the location of the boulder. For the cases of $\alpha \leq 90°$, the place where the decrease of overburden pressure occurred correlated well with the boulder location. However, when $\alpha > 90°$, removing the boulder caused decrease of overburden pressures in the range from −0.5D to 0.5D.

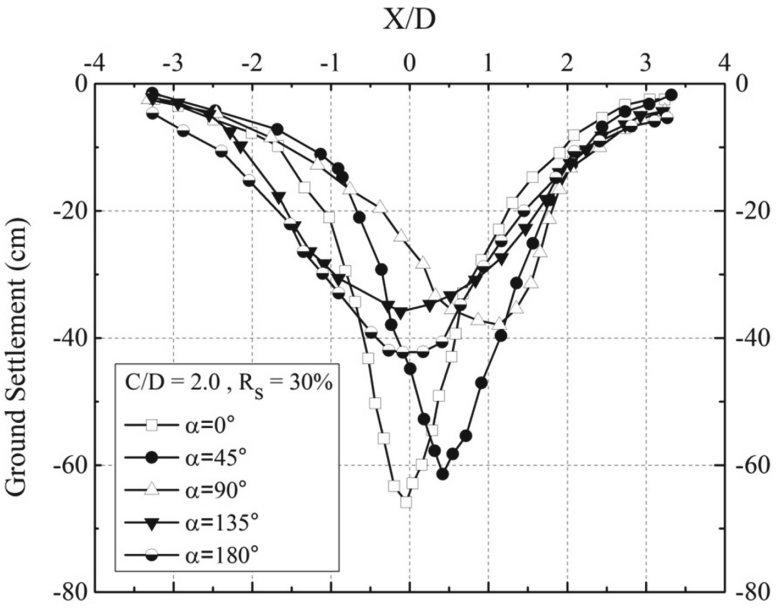

Fig. 4. Ground settlements for crushing the boulder at different locations.

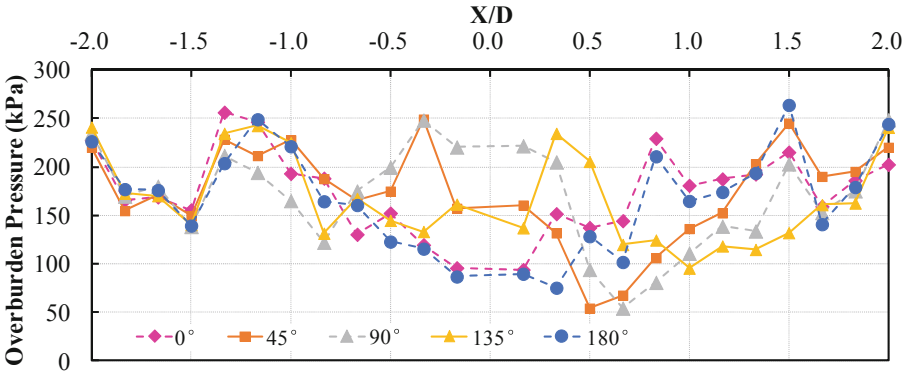

Fig. 5. Overburden pressures caused by crushing the boulder at different locations.

3.4 Bending Moments in Tunnel Lining

Figure 6 illustrates the distribution of bending moments in the tunnel lining when boulders at different locations were crushed and removed. Assuming the tunnel was a spherical ring and using force method, the distribution of bending moment in the lining would look like a peanut – negative moments on the crown and invert, and positive moments on the side walls (see the black line with circles in Fig. 6). Negative moments indicated the external side (in touch with the soils) of the lining was compressed by the

earth pressures and the internal side was tensioned. If volume loss was caused by crushing and removing the single boulder atop the tunnel crown ($\alpha = 0°$), distribution of bending moments exhibited a circular shape due to release of overburden pressures. When the location angle of boulder $\alpha = 45°$ and 90°, distribution of bending moments formed 'peanut' shape again. In the meantime, the right end of the peanut was elevated due to pressure release, and the left end was pushed down. The distribution of bending moments for $\alpha = 135°$ was mirror symmetric to the case of $\alpha = 45°$, since for both cases the horizontal coordinates of boulder location were the same. However, the magnitude of the bending moments was much larger for $\alpha = 135°$ case than that of $\alpha = 45°$ case. When the boulder below the tunnel invert was crushed and removed, the lateral earth pressures probably exceeded the overburden pressure and reaction of subgrade, and thus pushed the tunnel laterally and caused the distribution of bending moments to show '8' shape,

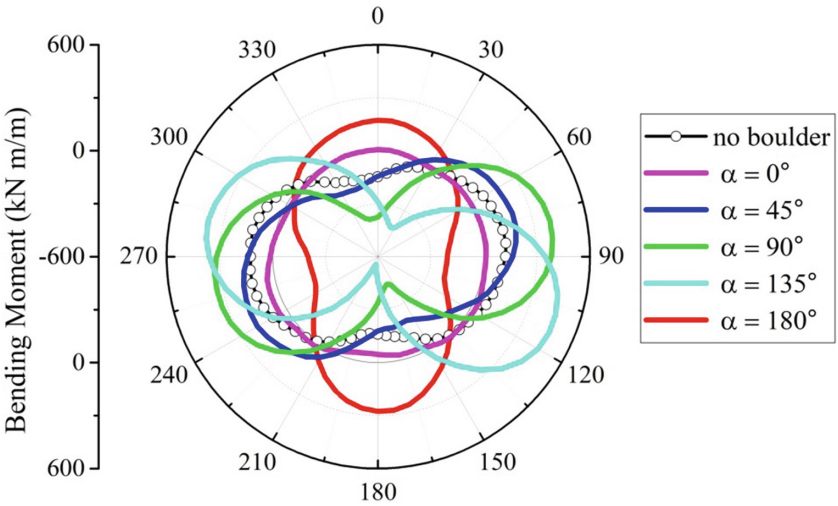

Fig. 6. Distribution of bending moments in the tunnel lining.

4 Conclusions

In this study, numerical simulations were carried out to investigate the influence of removing a single boulder located at different places around a tunnel, and the following conclusions can be reached:

1. Crushing and removing a boulder around a tunnel caused immediate volume loss. After installing the lining, sands fell into the cavity resulting disturbance to the surrounding stratum. The scope of falling zone moved up until it reached the ground surface which caused subsidence of ground surface.
2. The ground settlement trough reflected boulder location. Removing a boulder atop the tunnel crown caused the maximum ground subsidence but least extensive

influencing zone. If the boulder was located underneath the tunnel, the maximum settlements always occurred around the tunnel center.

3. Removal of the boulder resulted in decrease of overburden pressure around the location of the boulder. If the location angle of boulder α was less than 90°, the place where the decrease of overburden pressure occurred correlated well with the boulder location. However, when α was more than 90°, decrease of overburden pressure occurred within $\pm 0.5D$ away from tunnel center.
4. Other the case of a boulder locating above the tunnel crown, the distribution of bending moments exhibited 'peanut' shape of which the centerline oriented according to boulder location.

References

1. Hunt, S.W.: Tunneling in cobbles and boulders. In: Breakthroughs in Tunneling Short Course, Chicago IL, 14–16 August (2017)
2. Gu, L.: Qualifications for boulder breaking by shield machines and pre-treatment of boulders. Tunn. Constr. **26**(Suppl. 2), 12–13, 22 (2006). (In Chinese with English Abstract)
3. Wang, D.: Discussion about special investigation programs of spherical weathering in subway project. Guangzhou Arch. **39**(2), 42–46 (2011). (in Chinese with English Abstract)
4. Wang, P.: Treatment of boulders encountered in shield tunnelling under different geological conditions. Tunn. Constr. **32**(4), 571–575 (2012). (in Chinese with English Abstract)
5. Zhang, H., Chen, S., Tan, X., Zhao, Y.: Study on boulder treatment in shield tunnelling. Constr. Technol. **40**(350), 78–81 (2011). (in Chinese with English Abstract)
6. Cundall, P.A., Strack, O.D.L.: A discrete numerical model for granular assemblies. Géotechnique **29**(1), 47–65 (1979)
7. Lu, Y., Tan, Y., Li, X.: Stability analyses on slopes of clay-rock mixtures using discrete element method. Eng. Geol. **244**, 116–124 (2018)
8. Lu, Y., Tan, Y., Li, X., Liu, C.: Methodology for simulation of irregularly shaped gravel grains and its application to DEM modeling. J. Comput. Civil Eng. **31**(5), 04017023 (2017)